Check for updates

Article

MMS

Mathematics and Mechanics of Solids
2023, Vol. 28(5) 1113–1132
© The Author(s) 2022
Article reuse guidelines:
sagepub.com/journals-permissions
DOI: 10.1177/10812865221108997
journals.sagepub.com/home/mms
SAGE

Rayleigh waves in thermoelasticity: Triple porous media in local thermal non-equilibrium

Vittorio Zampoli
Department of Information and Electrical Engineering and Applied Mathematics, University of Salerno, Fisciano, Italy

Stan Chiriţă
Faculty of Mathematics, Alexandru Ioan Cuza University of Iaşi, Iaşi, Romania

Received 14 March 2022; accepted 7 June 2022

Abstract
Assuming the hypothesis of local thermal non-equilibrium, this work investigates the propagation of Rayleigh surface waves in a thermoelastic half-space, isotropic, homogeneous and structured with a triple level of porosity. Its surface is supposed to be stress-free, thermally insulated and characterized by null pressure boundary conditions. A class of wave solutions is highlighted for the differential system of the model, each solution satisfying suitable asymptotic conditions in the depth of the considered half-space. Then, the Rayleigh wave solution is sought as a linear combination of the elements of this class, and, moreover, by means of the selected boundary conditions, the associated secular equation is found. By solving the secular equation, the characteristics of the wave solution are determined: the propagation speed as well as the damping in time. With the purpose of clearly highlighting the characteristics of the model, the secular equation is solved numerically and significant graphical representations are provided, using the software packages Mathematica and MATLAB. This suggests an increase of the Rayleigh wave propagation speed, corroborated with the appearance of the damping in time of its amplitude.

Keywords
Triple porous media, local thermal non-equilibrium, Rayleigh surface waves, secular equation, propagation speed, time attenuation rate

1. Introduction

The main feature of the model investigated, with regard to its elastic component, is undoubtedly the presence of a triple level of porosity. On the basis of the pore sizes, it is possible to label porous media into three categories, namely, micro-porous materials (for which the pore sizes are less than 2nm), meso-porous materials (for which the pore sizes are 2–50 nm), and macro-porous materials (for which the pore sizes are greater than 50 nm). A good example of mineral structure showing simultaneously macro-,

Corresponding author:
Stan Chiriţă, Faculty of Mathematics, Alexandru Ioan Cuza University of Iaşi, Blvd. Carol I, no. 11, Iaşi 700506, Romania.
Email: schirita@uaic.ro

meso-, and micro-pores is given by clay, in which a coarser matrix of macro- and meso-pores can be detected at the level of interactions between particles while, in order to identify the micro-pores, it is necessary to go into more deep details of the material structure. Further explanations in this regard can be found in Heller-Kallai [1, see p. 415], where the relationship between water content in clay mineral aggregates and their (changing) porosity is well specified, as well as the effect of acid treatments able to increase the porosity.

The scope of applicability of porous materials certainly cannot be summed up in a few lines: thermal insulation, tissue engineering, and water purification represent just a few examples. Over the past decade, porous materials have been extensively studied, and various theories describing their thermodynamic behavior have been developed. Based on Darcy's law, and considering a single porosity structure, Biot [2–5] formulated the first deformation theory involving a porous elastic solid and a viscous compressible fluid. For the basic results, as well as for historical information about this founding theory, the reader can refer to the books by Cheng [6], Straughan [7], and Svanadze [8]. However, thinking about geological formations—for instance—it is easy to realize that they often show a variety of heterogeneous levels of porosity: fractures, fissures, cracks, and so on. Over the years, the porous matrix structure has thus evolved: Barenblatt and co-workers [9,10], resorting to the mixtures theory for modeling a fluid flow in a (rigid) fractured porous medium, have developed the double porosity model. As a natural consequence, the deformable skeleton with double porosity has been developed in the previous studies [11–16], while more recent results on double porous materials can be found in the previous studies [17–21]. As anticipated, a triple porous medium shows three contiguous levels of porosity: a main matrix, micro-fractures (less permeable), and macro-fractures (more permeable), coexisting and interacting with each other [22–25]. This is particularly interesting, e.g., in the context of fractured reservoirs. From the works by Shackelford [26], Gwo et al. [27], and Moutsopoulos et al. [28], one can get an idea of the different conductance and storage features exhibited by a triple porous material in each pore domain. Macro-pores are identifiable as primary flow paths, in which dispersion and convection are both prevalent; meso-pores locate the intermediate flow paths, where a predominance of the convection is observed; micro-pores define supplemental flow paths, as well as mass storage spaces where only the diffusive flow is meaningful. We must also mention the modeling of some biomechanical systems in clinical situations relating the bone, where several levels of porosity can exist: collagen-apatite porosity, lacunar–canalicular porosity, and intertrabecular porosity (see, e.g., Giorgio et al. [29,30]).

In parallel, we would like to mention that, dealing with petroleum engineering and hydrogeology, the knowledge of attenuation and dispersion of seismic waves linked to a wave-induced flow in porous rocks represents a fundamental tool in the assessment of reservoirs porosity and permeability (see, e.g., [31,32]). A variation in pore pressure, in the context of oil extraction or CO_2 storage, may induce a sudden seismicity or even slow subsidence and uplift phenomena. More generally, the pore pressure diffusion seems to be a triggering mechanism for earthquake swarms [33]. There is a huge interest toward the research in wave propagation in porous media, starting with Biot's early works [5,34,35], continuing with the studies by Wilson and Aifantis [12], Beskos et al. [14], Beskos and Papadakis [15], Shankland et al. [36], Berryman and Wang [37], and with more recent studies by Olny and Boutin [18], Müller et al. [31], Svanadze [38], Ciarletta et al. [39], Straughan [40], Davis et al. [41], Galeş and Chiriţă [42], Chiriţă and Arusoaie [43], and Chiriţă and Galeş [44]. Based on the results by Nield [45], Franchi et al. [46], and Svanadze [47], Chiriţă [48] develops a mathematical model able to describe the evolutive behavior of triple porous media under local thermal non-equilibrium hypothesis: taking into account anisotropic and inhomogeneous materials, the constitutive equations are given, showing the terms connecting pressures and temperatures at the different pore scales. The Lagrange identity method and the logarithmic convexity method are employed to investigate the basic initial boundary value problem; uniqueness and continuous dependence results are provided. For basic results and the current state of art for elastic Rayleigh surface waves, including the derivation of the classical Rayleigh equation as well as analysis of a surface wave of arbitrary profile, we recommend the recent work by Kaplunov and Prikazchikov [49].

Following Chiriţă [48], in this work, we drop the problem of Rayleigh surface wave propagation within the above triple porous matrix model in the framework of local thermal non-equilibrium. In this connection, we assume the half-space $x_2 > 0$, filled by a thermoelastic triple porous medium in local thermal non-equilibrium, to be free of supply loads, its surface $x_2 = 0$ to be free of mechanical traction, thermally insulated and with the pressure of pore network vanishing. In order to highlight the existence of

Rayleigh waves, we follow two steps: (1) first, we determine a class of wave solutions for the system of basic equations which satisfy suitable asymptotic conditions in the depth of the half-space, and then (2) we look for the Rayleigh surface wave solution as a linear combination of elements of the above-mentioned class that satisfy the assumed boundary conditions. In this way, we receive the secular equation that determines the features of the Rayleigh wave (propagation velocity and attenuation in time). The results obtained in this paper may be considered as more general in the sense that some other important formulas previously established by different authors may be deduced from our result as special cases. The results obtained are then applied to a specific triple porous material, namely, the Berea sandstone, solving the secular equation. We are able to show, both numerically and graphically, that the coupling between mechanical deformation, triple porous structure, and local thermal non-equilibrium results in an increase of the propagation velocity for the Rayleigh wave, as well as in the appearance of the damping in time of its amplitude.

We outline here that the methodology we are developing in solving the Rayleigh wave propagation problem includes mathematical results applicable to the general thermo-mechanical model, based on the search for wave solutions with assigned wavelength, and which leads to the general secular equation. But it also includes numerical methods for solving the secular equation involving the software packages Wolfram Mathematica and MathWorks MATLAB and the corresponding graphical methods.

We summarize the structure of the work. In section 2, under the assumption of local thermal non-equilibrium and following Chiriţă [48], the system of differential equations depicting the evolutive behavior of an isotropic, homogeneous triple porous medium is given, together with the main hypotheses on the characteristic coefficients. Section 3.1 defines the class of wave solutions of the basic differential system that satisfy the asymptotic conditions in the depth of the half-space. Section 3.2 is dedicated to finding the solution of the Rayleigh wave problem and, therefore, to establish the secular equation. Finally, in section 4, a numerical simulation of the results given in section 3.2 is proposed.

2. The triple porous model in local thermal non-equilibrium

The starting point is represented by the thermoelastic triple porous model under local thermal non-equilibrium given by Chiriţă [48]. We denote by $p_1(x,t)$ the fluid pressure at the macro-pores level; $p_2(x,t)$ is the fluid pressure at the level of meso-pores, while at the micro-pores level, the fluid pressure is labeled $p_3(x,t)$. Moreover, the three levels are assumed in local thermal non-equilibrium, so each of the three phases is characterized by its own temperature: $\theta_1(x,t)$ denotes the temperature in the macro-pores, the temperature in the meso-pores is given by $\theta_2(x,t)$ while that in the micro-pores is named $\theta_3(x,t)$. All of them are measured from the constant reference absolute temperature $T_0 > 0$. We identify a material point by its Cartesian coordinates, i.e., we set $x = (x_1, x_2, x_3)$. The common conventions for summation and differentiation are used. Latin subscripts and superscripts range in the set $\{1, 2, 3\}$, a sum is implied in case of repeated subscripts, and subscripts preceded by a comma mean partial differentiation with respect to that Cartesian coordinate; finally, superposed dots denote the time differentiation.

The basic equations in the case of an isotropic, homogeneous, triple porous thermoelastic medium in local thermal non-equilibrium (again, described in Chiriţă [48]) are the following. There, the elastic displacement components are u_r, the pressures in the macro-, meso- and micro-pores are p_r, and the temperatures θ_r are referred to the three phases:

$$\varrho \ddot{u}_n = \mu u_{n,mm} + (\lambda + \mu) u_{m,mn} - \beta_m p_{m,n} - \omega_m \theta_{m,n}, \tag{1}$$

$$a_{nm}\dot{p}_m + b_{nm}\dot{\theta}_m = k^{nm} p_{m,ll} - \beta_n \dot{u}_{m,m} - D_{nm} p_m, \tag{2}$$

$$b_{nm}\dot{p}_m + c_{nm}\dot{\theta}_m = \tfrac{1}{T_0} K^{nm} \theta_{m,ll} - \omega_n \dot{u}_{m,m} - \tfrac{1}{T_0} d_{nm} \theta_m, \tag{3}$$

for each $(x,t) = (x_1, x_2, x_3, t) \in B \times (0, \infty)$. The constant ϱ defines the reference mass density, while λ and μ are the first Lamé modulus and the shear modulus, respectively; β_n are Biot's parameters giving the pores compressibility, ω_n define the coefficients of thermal expansion for the three different phases, $a_{mn} = a_{nm}$ give a measure of the compressibility of the pore system, representing the components of the cross-coupling compressibility for the fluid flow at the level of interface between the three pore systems.

Again, $b_{mn} = b_{nm}$ are the components of the constitutive thermal tensor, $c_{mn} = c_{nm}$ give the heat capacity, and (d_{mn}) represents the internal heat transfer tensor defined as follows:

$$\mathbf{d} \equiv (d_{mn}) \equiv \begin{pmatrix} d_1 + d_2 & -d_1 & -d_2 \\ -d_1 & d_1 + d_3 & -d_3 \\ -d_2 & -d_3 & d_2 + d_3 \end{pmatrix}. \tag{4}$$

Furthermore, (D_{mn}) is defined as follows:

$$\mathbf{D} \equiv (D_{mn}) \equiv \begin{pmatrix} \gamma_1 + \gamma_2 & -\gamma_1 & -\gamma_2 \\ -\gamma_1 & \gamma_1 + \gamma_3 & -\gamma_3 \\ -\gamma_2 & -\gamma_3 & \gamma_2 + \gamma_3 \end{pmatrix}, \tag{5}$$

where γ_1, γ_2, and γ_3 are the leakage parameters, or even internal transport coefficients. Moreover, $k^{mn} = k'^{mn}/\mu'$, where μ' is the viscosity of the fluid and $k'^{mn} = k'^{nm}$ indicate the (macroscopic) intrinsic permeability connected to the three pore systems; $K^{mn} = K^{nm}$ are the components of the tensor of thermal conductivity.

Our analysis needs the following hypotheses on the above material coefficients:

H1. Elasticity set of hypotheses:

$$\mu > 0, \quad \lambda + 2\mu > 0, \quad \varrho > 0. \tag{6}$$

H2. Pores set of hypotheses:

$$k^{mn}\xi_m\xi_n > 0, \quad \text{for all} \quad (\xi_1, \xi_2, \xi_3) \neq 0; \tag{7}$$

$$\gamma_1 \geqslant 0, \quad \gamma_2 \geqslant 0, \quad \gamma_3 \geqslant 0. \tag{8}$$

H3. Thermal set of hypotheses:

$$K^{mn}\xi_m\xi_n > 0, \quad \text{for all} \quad (\xi_1, \xi_2, \xi_3) \neq 0; \tag{9}$$

$$d_1 \geqslant 0, \quad d_2 \geqslant 0, \quad d_3 \geqslant 0. \tag{10}$$

H4. Inertia/thermal capacity hypothesis: $f(p, \theta)$ defines a positive definite quadratic form:

$$\begin{gathered} f(p, \theta) \equiv a_{mn}p_m p_n + 2b_{mn}p_m\theta_n + c_{mn}\theta_m\theta_n > 0, \quad \text{for all} \\ p = (p_1, p_2, p_3) \neq 0 \quad \text{or} \quad \theta = (\theta_1, \theta_2, \theta_3) \neq 0. \end{gathered} \tag{11}$$

This last hypothesis implies that:

$$a_{mn}\xi_m\xi_n > 0, \quad \text{for all} \quad (\xi_1, \xi_2, \xi_3) \neq 0, \tag{12}$$

$$c_{mn}\xi_m\xi_n > 0, \quad \text{for all} \quad (\xi_1, \xi_2, \xi_3) \neq 0. \tag{13}$$

We prefer to introduce now the following notations, whose usefulness will be evident in the following:

$$c_1 = \sqrt{\frac{\lambda + 2\mu}{\varrho}}, \quad c_2 = \sqrt{\frac{\mu}{\varrho}}, \tag{14}$$

where c_1 and c_2 can represent, in the context of the classical elasticity, the propagation speeds of longitudinal and shear waves, respectively.

3. Rayleigh surface waves

The focus of the work is the study of the Rayleigh wave propagation problem applied to the model defined by the differential system (1)–(3). We then consider the half-space $x_2 > 0$ filled by a thermoelastic triple porous medium in local thermal non-equilibrium. The half-space is free of supply loads, and its surface $x_2 = 0$ is assumed free of any mechanical traction, thermally insulated and such that the pore system pressure is vanishing; furthermore, the surface wave is assumed to propagate in the half-space $x_2 \geqslant 0$ and in the x_1-axis direction. In the case of a triple porous, isotropic and homogeneous thermoelastic material in local thermal non-equilibrium, the Rayleigh wave propagation problem consists of finding wave-form solutions for the boundary value problem defined by the equations (1)–(3), the boundary conditions:

$$\begin{aligned} &t_{2n}(x_1, 0, x_3, t) = 0, \\ &p_n(x_1, 0, x_3, t) = 0, \\ &\theta_n(x_1, 0, x_3, t) = 0, \quad \text{for all} \quad x_1, x_3 \in \mathbb{R},\, t \geqslant 0, \end{aligned} \tag{15}$$

and the following asymptotic conditions:

$$\begin{aligned} &\lim_{x_2 \to \infty} u_n(x_1, x_2, x_3, t) = 0, \quad \lim_{x_2 \to \infty} t_{mn}(x_1, x_2, x_3, t) = 0, \\ &\lim_{x_2 \to \infty} p_n(x_1, x_2, x_3, t) = 0, \\ &\lim_{x_2 \to \infty} \theta_n(x_1, x_2, x_3, t) = 0, \quad \text{for all} \quad x_1, x_3 \in \mathbb{R},\, t \geqslant 0, \end{aligned} \tag{16}$$

where t_{mn}, defined as follows:

$$t_{mn} = 2\mu e_{mn} + \lambda e_{ll}\delta_{mn} - \beta_l p_l \delta_{mn} - \omega_l \theta_l \delta_{mn}, \quad e_{mn} = \frac{1}{2}(u_{m,n} + u_{n,m}), \tag{17}$$

are the components of the stress tensor.

In what follows, we proceed to solve the Rayleigh wave propagation problem. For this purpose, we highlight a class of wave solutions for the basic system (1)–(3) which, in addition, satisfy the asymptotic conditions (16). Then, we express the solution of our problem in terms of elements of this class.

3.1. A class of wave solutions for the basic differential system

We assume waves propagating along the x_1-axis. Solutions in wave form (of assigned wavelength) are then sought for the differential system (1)–(3), i.e.,

$$\begin{aligned} u_1(x_1, x_2, x_3, t) &= \mathrm{Re}\left\{\tfrac{i}{\varkappa}\, U_1\, e^{i\varkappa(x_1 - \upsilon t + r x_2)}\right\}, \\ u_2(x_1, x_2, x_3, t) &= \mathrm{Re}\left\{\tfrac{i}{\varkappa}\, U_2\, e^{i\varkappa(x_1 - \upsilon t + r x_2)}\right\}, \\ u_3(x_1, x_2, x_3, t) &= 0, \\ p_1(x_1, x_2, x_3, t) &= \mathrm{Re}\left\{c_1 \sqrt{\tfrac{\varrho}{a_{11}}} P_1\, e^{i\varkappa(x_1 - \upsilon t + r x_2)}\right\}, \\ p_2(x_1, x_2, x_3, t) &= \mathrm{Re}\left\{c_1 \sqrt{\tfrac{\varrho}{a_{22}}} P_2\, e^{i\varkappa(x_1 - \upsilon t + r x_2)}\right\}, \\ p_3(x_1, x_2, x_3, t) &= \mathrm{Re}\left\{c_1 \sqrt{\tfrac{\varrho}{a_{33}}} P_3\, e^{i\varkappa(x_1 - \upsilon t + r x_2)}\right\}, \\ \theta_n(x_1, x_2, x_3, t) &= \mathrm{Re}\left\{T_0\, T_n\, e^{i\varkappa(x_1 - \upsilon t + r x_2)}\right\}, \end{aligned} \tag{18}$$

where $i = \sqrt{-1}$ represents the imaginary unit, $\mathrm{Re}\{\cdot\}$ stands for the real part, $\varkappa > 0$ is the wave number (assumed real), and $\{U_1, U_2, P_1, P_2, P_3, T_1, T_2, T_3\}$ denotes a non-zero complex constant vector; moreover, υ is a parameter (assumed complex) such that the wave speed is given by $\mathrm{Re}(\upsilon) \geqslant 0$ and the damping in time of the wave is given by $\exp[\varkappa \mathrm{Im}(\upsilon) t]$, provided that $\mathrm{Im}(\upsilon) \leqslant 0$ in order to ensure wave solutions with finite internal energy. We are then interested in wave solutions of the form (18) with:

$$\mathrm{Re}(\upsilon) \geqslant 0, \tag{19}$$

and

$$\mathrm{Im}(v) \leqslant 0. \tag{20}$$

It is easy to infer that the condition $\mathrm{Re}\,(v) = 0$ denotes a standing wave; in contrast, when $\mathrm{Re}\,(v) > 0$, we have a genuine harmonic in time wave. In addition, $\mathrm{Im}\,(v) = 0$ returns a wave undamped in time, while the damping in time is highlighted by the condition $\mathrm{Im}\,(v) > 0$.

We point out that the asymptotic conditions (16) give the following constraint on the complex parameter r:

$$\mathrm{Im}(r) > 0. \tag{21}$$

Therefore, we have to determine the complex parameter $r = r(v)$ in such a way that the restriction (21) is fulfilled, and equation (18) satisfies the differential system (1)–(3).

By substituting equation (18) in system (1), we receive the algebraic system:

$$\begin{aligned}&(\lambda + 2\mu - \varrho v^2 + \mu r^2)U_1 + (\lambda + \mu) r U_2 + \beta_1 c_1 \sqrt{\tfrac{\varrho}{a_{11}}} P_1 + \beta_2 c_1 \sqrt{\tfrac{\varrho}{a_{22}}} P_2 + \beta_3 c_1 \sqrt{\tfrac{\varrho}{a_{33}}} P_3 \\ &+ \omega_1 T_0 T_1 + \omega_2 T_0 T_2 + \omega_3 T_0 T_3 = 0,\end{aligned} \tag{22}$$

and

$$\begin{aligned}&(\lambda + \mu) r U_1 + [(\lambda + 2\mu) r^2 + \mu - \varrho v^2] U_2 + \beta_1 c_1 \sqrt{\tfrac{\varrho}{a_{11}}} r P_1 + \beta_2 c_1 \sqrt{\tfrac{\varrho}{a_{22}}} r P_2 + \beta_3 c_1 \sqrt{\tfrac{\varrho}{a_{33}}} r P_3 \\ &+ \omega_1 T_0 r T_1 + \omega_2 T_0 r T_2 + \omega_3 T_0 r T_3 = 0.\end{aligned} \tag{23}$$

By appropriate combinations of the above two equations and using the following notations:

$$\begin{aligned}&s^2 = 1 + r^2, \quad V = r U_1 - U_2, \quad W = U_1 + r U_2, \\ &w = -\frac{v}{c_1} i,\end{aligned} \tag{24}$$

we get:

$$\left(s^2 + \frac{c_1^2}{c_2^2} w^2\right) V = 0, \tag{25}$$

and

$$\begin{aligned}\left(s^2 + w^2\right) W + \frac{\beta_1}{c_1 \sqrt{\varrho a_{11}}} s^2 P_1 + \frac{\beta_2}{c_1 \sqrt{\varrho a_{22}}} s^2 P_2 + \frac{\beta_3}{c_1 \sqrt{\varrho a_{33}}} s^2 P_3 \\ + \frac{\omega_1 T_0}{\varrho c_1^2} s^2 T_1 + \frac{\omega_2 T_0}{\varrho c_1^2} s^2 T_2 + \frac{\omega_3 T_0}{\varrho c_1^2} s^2 T_3 = 0.\end{aligned} \tag{26}$$

Again, from equations (2), (3), and (18) and resorting to the variable w given in equation (24), we obtain the following algebraic systems, useful for the determination of the unknown quantities W, P_1, P_2, P_3, T_1, T_2, T_3:

$$\begin{aligned}&-\frac{\beta_1 w}{\varkappa k^{11}} \sqrt{\frac{a_{11}}{\varrho}} W + \left(s^2 + \frac{D_{11}}{\varkappa^2 k^{11}} + \frac{a_{11} c_1}{\varkappa k^{11}} w\right) P_1 + \left(\frac{k^{12}}{k^{11}} s^2 + \frac{D_{12}}{\varkappa^2 k^{11}}\right. \\ &\left. + \frac{a_{12} c_1}{\varkappa k^{11}} w\right) \sqrt{\frac{a_{11}}{a_{22}}} P_2 + \left(\frac{k^{13}}{k^{11}} s^2 + \frac{D_{13}}{\varkappa^2 k^{11}} + \frac{a_{13} c_1}{\varkappa k^{11}} w\right) \sqrt{\frac{a_{11}}{a_{33}}} P_3 \\ &+ \frac{b_{11} T_0}{\varkappa k^{11}} \sqrt{\frac{a_{11}}{\varrho}} w T_1 + \frac{b_{12} T_0}{\varkappa k^{11}} \sqrt{\frac{a_{11}}{\varrho}} w T_2 + \frac{b_{13} T_0}{\varkappa k^{11}} \sqrt{\frac{a_{11}}{\varrho}} w T_3 = 0,\end{aligned}$$

$$
\begin{aligned}
&-\frac{\beta_2 w}{\varkappa k^{22}}\sqrt{\frac{a_{22}}{\varrho}}W+\left(\frac{k^{21}}{k^{22}}s^2+\frac{D_{21}}{\varkappa^2 k^{22}}+\frac{a_{21}c_1}{\varkappa k^{22}}w\right)\sqrt{\frac{a_{22}}{a_{11}}}P_1+\left(s^2+\frac{D_{22}}{\varkappa^2 k^{22}}\right.\\
&\left.+\frac{a_{22}c_1}{\varkappa k^{22}}w\right)P_2+\left(\frac{k^{23}}{k^{22}}s^2+\frac{D_{23}}{\varkappa^2 k^{22}}+\frac{a_{23}c_1}{\varkappa k^{22}}w\right)\sqrt{\frac{a_{22}}{a_{33}}}P_3\\
&+\frac{b_{21}T_0}{\varkappa k^{22}}\sqrt{\frac{a_{22}}{\varrho}}wT_1+\frac{b_{22}T_0}{\varkappa k^{22}}\sqrt{\frac{a_{22}}{\varrho}}wT_2+\frac{b_{23}T_0}{\varkappa k^{22}}\sqrt{\frac{a_{22}}{\varrho}}wT_3=0,\\
&-\frac{\beta_3 w}{\varkappa k^{33}}\sqrt{\frac{a_{33}}{\varrho}}W+\left(\frac{k^{31}}{k^{33}}s^2+\frac{D_{31}}{\varkappa^2 k^{33}}+\frac{a_{31}c_1}{\varkappa k^{33}}w\right)\sqrt{\frac{a_{33}}{a_{11}}}P_1+\left(\frac{k^{32}}{k^{33}}s^2+\frac{D_{32}}{\varkappa^2 k^{33}}\right.\\
&\left.+\frac{a_{32}c_1}{\varkappa k^{33}}w\right)\sqrt{\frac{a_{33}}{a_{22}}}P_2+\left(s^2+\frac{D_{33}}{\varkappa^2 k^{33}}+\frac{a_{33}c_1}{\varkappa k^{33}}w\right)P_3\\
&+\frac{b_{31}T_0}{\varkappa k^{33}}\sqrt{\frac{a_{33}}{\varrho}}wT_1+\frac{b_{32}T_0}{\varkappa k^{33}}\sqrt{\frac{a_{33}}{\varrho}}wT_2+\frac{b_{33}T_0}{\varkappa k^{33}}\sqrt{\frac{a_{33}}{\varrho}}wT_3=0,
\end{aligned}
\tag{27}
$$

and

$$
\begin{aligned}
&-\frac{\omega_1 c_1 w}{\varkappa K^{11}}W+\frac{b_{11}c_1^2}{\varkappa K^{11}}\sqrt{\frac{\varrho}{a_{11}}}wP_1+\frac{b_{12}c_1^2}{\varkappa K^{11}}\sqrt{\frac{\varrho}{a_{22}}}wP_2+\frac{b_{13}c_1^2}{\varkappa K^{11}}\sqrt{\frac{\varrho}{a_{33}}}wP_3\\
&+\left(s^2+\frac{d_{11}}{\varkappa^2 K^{11}}+\frac{c_{11}c_1T_0}{\varkappa K^{11}}w\right)T_1+\left(\frac{K^{12}}{K^{11}}s^2+\frac{d_{12}}{\varkappa^2 K^{11}}+\frac{c_{12}c_1T_0}{\varkappa K^{11}}w\right)T_2\\
&+\left(\frac{K^{13}}{K^{11}}s^2+\frac{d_{13}}{\varkappa^2 K^{11}}+\frac{c_{13}c_1T_0}{\varkappa K^{11}}w\right)T_3=0,\\
&-\frac{\omega_2 c_1 w}{\varkappa K^{22}}W+\frac{b_{21}c_1^2}{\varkappa K^{22}}\sqrt{\frac{\varrho}{a_{11}}}wP_1+\frac{b_{22}c_1^2}{\varkappa K^{22}}\sqrt{\frac{\varrho}{a_{22}}}wP_2+\frac{b_{23}c_1^2}{\varkappa K^{22}}\sqrt{\frac{\varrho}{a_{33}}}wP_3\\
&+\left(\frac{K^{21}}{K^{22}}s^2+\frac{d_{21}}{\varkappa^2 K^{22}}+\frac{c_{21}c_1T_0}{\varkappa K^{22}}w\right)T_1+\left(s^2+\frac{d_{22}}{\varkappa^2 K^{22}}+\frac{c_{22}c_1T_0}{\varkappa K^{22}}w\right)T_2\\
&+\left(\frac{K^{23}}{K^{22}}s^2+\frac{d_{23}}{\varkappa^2 K^{22}}+\frac{c_{23}c_1T_0}{\varkappa K^{22}}w\right)T_3=0,\\
&-\frac{\omega_3 c_1 w}{\varkappa K^{33}}W+\frac{b_{31}c_1^2}{\varkappa K^{33}}\sqrt{\frac{\varrho}{a_{11}}}wP_1+\frac{b_{32}c_1^2}{\varkappa K^{33}}\sqrt{\frac{\varrho}{a_{22}}}wP_2+\frac{b_{33}c_1^2}{\varkappa K^{33}}\sqrt{\frac{\varrho}{a_{33}}}wP_3\\
&+\left(\frac{K^{31}}{K^{33}}s^2+\frac{d_{31}}{\varkappa^2 K^{33}}+\frac{c_{31}c_1T_0}{\varkappa K^{33}}w\right)T_1+\left(\frac{K^{32}}{K^{33}}s^2+\frac{d_{32}}{\varkappa^2 K^{33}}+\frac{c_{32}c_1T_0}{\varkappa K^{33}}w\right)T_2\\
&+\left(s^2+\frac{d_{33}}{\varkappa^2 K^{33}}+\frac{c_{33}c_1T_0}{\varkappa K^{33}}w\right)T_3=0.
\end{aligned}
\tag{28}
$$

Therefore, the algebraic system defined by relations (25)–(28), in terms of the unknown variables V, W, P_1, P_2, P_3, T_1, T_2, T_3, admits non-trivial solutions, and so its discriminant has to be null, i.e.,

$$
\left(s^2+\frac{c_1^2}{c_2^2}w^2\right)\det\big(\pi(s^2)\big)=0,
\tag{29}
$$

where $\pi(s^2)$ is the 7×7 matrix:

$$
\pi(s^2)\equiv\big(\pi_{MN}(s^2)\big)_{(7\times 7)},
\tag{30}
$$

having its elements $\pi_{MN}(s^2)$, $M, N = 1, 2, ..., 7$, defined as in Appendix 1. We denote by $s_1^2, s_2^2, \ldots, s_7^2$, the roots of the equation:

$$\det\left(\pi(s^2)\right) = 0, \tag{31}$$

and we set:

$$r_M = i\sqrt{1 - s_M^2}, \quad M = 1, 2, ..., 7. \tag{32}$$

Furthermore, the relations (25) and (29) give the root $s^2 = s_8^2$, with the corresponding $V = V^{(8)}$, and

$$s_8^2 = -\frac{c_1^2}{c_2^2} w^2, \quad V^{(8)} = 1, \tag{33}$$

and hence, we set:

$$r_8 = i\sqrt{1 - s_8^2} = i\sqrt{1 + \frac{c_1^2}{c_2^2} w^2} = i\sqrt{1 - \frac{v^2}{c_2^2}}. \tag{34}$$

Therefore, for

$$r_1 = i\sqrt{1 - s_1^2}, \tag{35}$$

we deduce the following solution:

$$\begin{aligned} &U_1^{(1)} = \frac{1}{s_1^2}, \quad U_2^{(1)} = \frac{r_1}{s_1^2}, \\ &P_1^{(1)} = \frac{\pi_{21}^*(s_1^2)}{\pi_{11}^*(s_1^2)}, P_2^{(1)} = \frac{\pi_{31}^*(s_1^2)}{\pi_{11}^*(s_1^2)}, P_3^{(1)} = \frac{\pi_{41}^*(s_1^2)}{\pi_{11}^*(s_1^2)}, \\ &T_1^{(1)} = \frac{\pi_{51}^*(s_1^2)}{\pi_{11}^*(s_1^2)}, T_2^{(1)} = \frac{\pi_{61}^*(s_1^2)}{\pi_{11}^*(s_1^2)}, T_3^{(1)} = \frac{\pi_{71}^*(s_1^2)}{\pi_{11}^*(s_1^2)}; \end{aligned} \tag{36}$$

for

$$r_2 = i\sqrt{1 - s_2^2}, \tag{37}$$

we deduce the following solution:

$$\begin{aligned} &U_1^{(2)} = \frac{1}{s_2^2}\frac{\pi_{12}^*(s_2^2)}{\pi_{22}^*(s_2^2)}, \quad U_2^{(2)} = \frac{r_2}{s_2^2}\frac{\pi_{12}^*(s_2^2)}{\pi_{22}^*(s_2^2)}, \\ &P_1^{(2)} = 1, \; P_2^{(2)} = \frac{\pi_{32}^*(s_2^2)}{\pi_{22}^*(s_2^2)}, \; P_3^{(2)} = \frac{\pi_{42}^*(s_2^2)}{\pi_{22}^*(s_2^2)}, \\ &T_1^{(2)} = \frac{\pi_{52}^*(s_2^2)}{\pi_{22}^*(s_2^2)}, \; T_2^{(2)} = \frac{\pi_{62}^*(s_2^2)}{\pi_{22}^*(s_2^2)}, \; T_3^{(2)} = \frac{\pi_{72}^*(s_2^2)}{\pi_{22}^*(s_2^2)}; \end{aligned} \tag{38}$$

for

$$r_3 = i\sqrt{1 - s_3^2}, \tag{39}$$

we deduce the following solution:

$$\begin{aligned}
&U_1^{(3)} = \frac{1}{s_3^2}\frac{\pi_{13}^*(s_3^2)}{\pi_{33}^*(s_3^2)}, \quad U_2^{(3)} = \frac{r_3}{s_3^2}\frac{\pi_{13}^*(s_3^2)}{\pi_{33}^*(s_3^2)},\\
&P_1^{(3)} = \frac{\pi_{23}^*(s_3^2)}{\pi_{33}^*(s_3^2)}, \; P_2^{(3)} = 1, \; P_3^{(3)} = \frac{\pi_{43}^*(s_3^2)}{\pi_{33}^*(s_3^2)},\\
&T_1^{(3)} = \frac{\pi_{53}^*(s_3^2)}{\pi_{33}^*(s_3^2)}, \; T_2^{(3)} = \frac{\pi_{63}^*(s_3^2)}{\pi_{33}^*(s_3^2)}, \; T_3^{(3)} = \frac{\pi_{73}^*(s_3^2)}{\pi_{33}^*(s_3^2)};
\end{aligned} \tag{40}$$

for

$$r_4 = i\sqrt{1 - s_4^2}, \tag{41}$$

we deduce the following solution:

$$\begin{aligned}
&U_1^{(4)} = \frac{1}{s_4^2}\frac{\pi_{14}^*(s_4^2)}{\pi_{44}^*(s_4^2)}, \quad U_2^{(4)} = \frac{r_4}{s_4^2}\frac{\pi_{14}^*(s_4^2)}{\pi_{44}^*(s_4^2)},\\
&P_1^{(4)} = \frac{\pi_{24}^*(s_4^2)}{\pi_{44}^*(s_4^2)}, \; P_2^{(4)} = \frac{\pi_{34}^*(s_4^2)}{\pi_{44}^*(s_4^2)}, \; P_3^{(4)} = 1,\\
&T_1^{(4)} = \frac{\pi_{54}^*(s_4^2)}{\pi_{44}^*(s_4^2)}, \; T_2^{(4)} = \frac{\pi_{64}^*(s_4^2)}{\pi_{44}^*(s_4^2)}, \; T_3^{(4)} = \frac{\pi_{74}^*(s_4^2)}{\pi_{44}^*(s_4^2)};
\end{aligned} \tag{42}$$

for

$$r_5 = i\sqrt{1 - s_5^2}, \tag{43}$$

we deduce the following solution:

$$\begin{aligned}
&U_1^{(5)} = \frac{1}{s_5^2}\frac{\pi_{15}^*(s_5^2)}{\pi_{55}^*(s_5^2)}, \quad U_2^{(5)} = \frac{r_5}{s_5^2}\frac{\pi_{15}^*(s_5^2)}{\pi_{55}^*(s_5^2)},\\
&P_1^{(5)} = \frac{\pi_{25}^*(s_5^2)}{\pi_{55}^*(s_5^2)}, \; P_2^{(5)} = \frac{\pi_{35}^*(s_5^2)}{\pi_{55}^*(s_5^2)}, \; P_3^{(5)} = \frac{\pi_{45}^*(s_5^2)}{\pi_{55}^*(s_5^2)},\\
&T_1^{(5)} = 1, \; T_2^{(5)} = \frac{\pi_{65}^*(s_5^2)}{\pi_{55}^*(s_5^2)}, \; T_3^{(5)} = \frac{\pi_{75}^*(s_5^2)}{\pi_{55}^*(s_5^2)};
\end{aligned} \tag{44}$$

for

$$r_6 = i\sqrt{1 - s_6^2}, \tag{45}$$

we deduce the following solution:

$$\begin{aligned}
&U_1^{(6)} = \frac{1}{s_6^2}\frac{\pi_{16}^*(s_6^2)}{\pi_{66}^*(s_6^2)}, \quad U_2^{(6)} = \frac{r_6}{s_6^2}\frac{\pi_{16}^*(s_6^2)}{\pi_{66}^*(s_6^2)},\\
&P_1^{(6)} = \frac{\pi_{26}^*(s_6^2)}{\pi_{66}^*(s_6^2)}, \; P_2^{(6)} = \frac{\pi_{36}^*(s_6^2)}{\pi_{66}^*(s_6^2)}, \; P_3^{(6)} = \frac{\pi_{46}^*(s_6^2)}{\pi_{66}^*(s_6^2)},\\
&T_1^{(6)} = \frac{\pi_{56}^*(s_6^2)}{\pi_{66}^*(s_6^2)}, \; T_2^{(6)} = 1, \; T_3^{(6)} = \frac{\pi_{76}^*(s_6^2)}{\pi_{66}^*(s_6^2)};
\end{aligned} \tag{46}$$

for

$$r_7 = i\sqrt{1 - s_7^2}, \tag{47}$$

we deduce the following solution:

$$\begin{aligned} U_1^{(7)} &= \frac{1}{s_7^2}\frac{\pi_{17}^*(s_7^2)}{\pi_{77}^*(s_7^2)}, \quad U_2^{(7)} = \frac{r_7}{s_7^2}\frac{\pi_{17}^*(s_7^2)}{\pi_{77}^*(s_7^2)}, \\ P_1^{(7)} &= \frac{\pi_{27}^*(s_7^2)}{\pi_{77}^*(s_7^2)}, \; P_2^{(7)} = \frac{\pi_{37}^*(s_7^2)}{\pi_{77}^*(s_7^2)}, \; P_3^{(7)} = \frac{\pi_{47}^*(s_7^2)}{\pi_{77}^*(s_7^2)}, \\ T_1^{(7)} &= \frac{\pi_{57}^*(s_7^2)}{\pi_{77}^*(s_7^2)}, \; T_2^{(7)} = \frac{\pi_{67}^*(s_7^2)}{\pi_{77}^*(s_7^2)}, \; T_3^{(7)} = 1; \end{aligned} \tag{48}$$

and for

$$r_8 = i\sqrt{1 - s_8^2} = i\sqrt{1 + \frac{c_1^2}{c_2^2}w^2} = i\sqrt{1 - \frac{\upsilon^2}{c_2^2}}, \tag{49}$$

we deduce the following solution:

$$\begin{aligned} U_1^{(8)} &= \frac{r_8}{s_8^2}, \quad U_2^{(8)} = -\frac{1}{s_8^2}, \\ P_1^{(8)} &= P_2^{(8)} = P_3^{(8)} = 0, \quad T_1^{(8)} = T_2^{(8)} = T_3^{(8)} = 0. \end{aligned} \tag{50}$$

Here, we have denoted by $\pi_{MN}^*(s^2)$, $M, N = 1, 2, ..., 7$, the elements of the adjoint matrix $\boldsymbol{\pi}^*(s^2)$ related to the previous matrix $\boldsymbol{\pi}(s^2)$.

At this point, one has to remember that the eight wave solutions (18) in which we have set $\mathcal{U} = \mathcal{U}^{(M)}, \quad M = 1, 2, ..., 8,$ where $\mathcal{U} \equiv \{U_1, U_2, P_1, P_2, P_3, T_1, T_2, T_3\}$ and $\mathcal{U}^{(M)} \equiv \{U_1^{(M)}, U_2^{(M)}, P_1^{(M)}, P_2^{(M)}, P_3^{(M)}, T_1^{(M)}, T_2^{(M)}, T_3^{(M)}\}$, $M = 1, 2, ..., 8$, given by the relations (35)–(50), satisfy the basic equations (1)–(3) as well as the asymptotic conditions (16), for any value of υ (or w).

3.2. Rayleigh wave solution

The treatment of the Rayleigh wave propagation problem implies that we have to search its solution as a linear combination of the eight solutions of the previous section, that is we seek the solution in the form:

$$\begin{aligned} u_1(x_1, x_2, x_3, t) &= \mathrm{Re}\left\{\frac{i}{\varkappa}\, e^{i\varkappa(x_1 - \upsilon t)} \sum_{M=1}^{8} A_M U_1^{(M)} e^{i\varkappa r_M x_2}\right\}, \\ u_2(x_1, x_2, x_3, t) &= \mathrm{Re}\left\{\frac{i}{\varkappa}\, e^{i\varkappa(x_1 - \upsilon t)} \sum_{M=1}^{8} A_M U_2^{(M)} e^{i\varkappa r_M x_2}\right\}, \\ u_3(x_1, x_2, x_3, t) &= 0, \\ p_1(x_1, x_2, x_3, t) &= \mathrm{Re}\left\{c_1\sqrt{\frac{\varrho}{a_{11}}} e^{i\varkappa(x_1 - \upsilon t)} \sum_{M=1}^{8} A_M P_1^{(M)} e^{i\varkappa r_M x_2}\right\}, \end{aligned} \tag{51}$$

$$
\begin{aligned}
p_2(x_1,x_2,x_3,t) &= \mathrm{Re}\left\{ c_1\sqrt{\frac{\varrho}{a_{22}}}e^{i\varkappa(x_1-vt)}\sum_{M=1}^{8} A_M P_2^{(M)} e^{i\varkappa r_M x_2}\right\},\\
p_3(x_1,x_2,x_3,t) &= \mathrm{Re}\left\{ c_1\sqrt{\frac{\varrho}{a_{33}}}e^{i\varkappa(x_1-vt)}\sum_{M=1}^{8} A_M P_3^{(M)} e^{i\varkappa r_M x_2}\right\},\\
\theta_n(x_1,x_2,x_3,t) &= T_0\mathrm{Re}\left\{ e^{i\varkappa(x_1-vt)}\sum_{M=1}^{8} A_M T_n^{(M)} e^{i\varkappa r_M x_2}\right\},
\end{aligned}
\tag{51}
$$

where $A_1, A_2, ..., A_8$ are the constant parameters, and at least one of them is different from zero. They are determined in such a way that the boundary conditions (15) hold true, and with $\mathcal{U}^{(M)} \equiv \{U_1^{(M)}, U_2^{(M)}, P_1^{(M)}, P_2^{(M)}, P_3^{(M)}, T_1^{(M)}, T_2^{(M)}, T_3^{(M)}\}$, $M = 1, 2, ..., 8$, given by relations (36)–(50). We have to remember that the system of functions (51) satisfies the basic equations (1)–(3) as well as the asymptotic conditions (16), for any value of v. In the following, we determine the unknown complex parameter v and the unknown parameters $A_1, A_2, ..., A_8$, not all null, so that the boundary conditions (15) are fulfilled. Therefore, using the system of functions (51) in the constitutive equation (17) and in the boundary conditions (15), we obtain for the determination of the unknown parameters $A_1, A_2, ..., A_8$, the following homogeneous algebraic system:

$$
\begin{cases}
\sum\limits_{M=1}^{8} S_{21}^{(M)} A_M = 0,\\
\sum\limits_{M=1}^{8} S_{22}^{(M)} A_M = 0,\\
\sum\limits_{M=1}^{8} P_n^{(M)} A_M = 0,\\
\sum\limits_{M=1}^{8} T_n^{(M)} A_M = 0, \quad n = 1, 2, 3,
\end{cases}
\tag{52}
$$

with

$$
\begin{aligned}
S_{21}^{(M)} &= r_M U_1^{(M)} + U_2^{(M)},\\
S_{22}^{(M)} &= \left(1 - \frac{2c_2^2}{c_1^2}\right) U_1^{(M)} + r_M U_2^{(M)}, \quad M = 1, 2, ..., 8.
\end{aligned}
\tag{53}
$$

Since we are looking for non-trivial solutions for the Rayleigh wave propagation problem in the form (51), the algebraic system (52) has to have non-trivial solutions. That means we have its discriminant to be vanishing and, therefore, we are led to the following secular equation for the determination of the complex parameter v (or w):

$$
\begin{vmatrix}
E(r_1,s_1) & E(r_2,s_2) & E(r_3,s_3) & E(r_4,s_4) & E(r_5,s_5) & E(r_6,s_6) & E(r_7,s_7)\\
\pi_{21}^*(s_1^2) & \pi_{22}^*(s_2^2) & \pi_{23}^*(s_3^2) & \pi_{24}^*(s_4^2) & \pi_{25}^*(s_5^2) & \pi_{26}^*(s_6^2) & \pi_{27}^*(s_7^2)\\
\pi_{31}^*(s_1^2) & \pi_{32}^*(s_2^2) & \pi_{33}^*(s_3^2) & \pi_{34}^*(s_4^2) & \pi_{35}^*(s_5^2) & \pi_{36}^*(s_6^2) & \pi_{37}^*(s_7^2)\\
\pi_{41}^*(s_1^2) & \pi_{42}^*(s_2^2) & \pi_{43}^*(s_3^2) & \pi_{44}^*(s_4^2) & \pi_{45}^*(s_5^2) & \pi_{46}^*(s_6^2) & \pi_{47}^*(s_7^2)\\
\pi_{51}^*(s_1^2) & \pi_{52}^*(s_2^2) & \pi_{53}^*(s_3^2) & \pi_{54}^*(s_4^2) & \pi_{55}^*(s_5^2) & \pi_{56}^*(s_6^2) & \pi_{57}^*(s_7^2)\\
\pi_{61}^*(s_1^2) & \pi_{62}^*(s_2^2) & \pi_{63}^*(s_3^2) & \pi_{64}^*(s_4^2) & \pi_{65}^*(s_5^2) & \pi_{66}^*(s_6^2) & \pi_{67}^*(s_7^2)\\
\pi_{71}^*(s_1^2) & \pi_{72}^*(s_2^2) & \pi_{73}^*(s_3^2) & \pi_{74}^*(s_4^2) & \pi_{75}^*(s_5^2) & \pi_{76}^*(s_6^2) & \pi_{77}^*(s_7^2)
\end{vmatrix} = 0,
\tag{54}
$$

where

$$
E(r_k,s_k) = \pi_{kk}^*(s_k^2)\left[S_{22}^{(k)} S_{21}^{(8)} - S_{22}^{(8)} S_{21}^{(k)}\right], \quad \text{not summed on } k, \quad k = 1, 2, ..., 7,
\tag{55}
$$

and, moreover, in view of relations (36)–(50) and (53) and (55), we have:

$$E(r_k, s_k) = \frac{c_2^2 \pi_{1k}^*(s_k^2)}{c_1^2 s_8^2 s_k^2} \left[\left(2 - s_8^2\right) \left(2 - \frac{c_1^2}{c_2^2} s_k^2\right) + 4 r_k r_8 \right], \quad \text{not summed on } k, \quad k = 1, 2, ..., 7. \tag{56}$$

A brief look at the relations defining the elements of the determinant describing the secular equation (54) shows that these elements are dependent on w. This means that the secular equation (54) is an algebraic equation in terms of w, subjected to the restrictions given by the following:

$$\mathrm{Re}\,(w) \leqslant 0, \quad \mathrm{Im}(w) \leqslant 0, \tag{57}$$

and the restrictions imposed by the relation (21). As a consequence, we have to get roots w of the secular equation (54) fulfilling the restrictions (57) and which make:

$$\mathrm{Im}\,(r_k(w)) > 0, \quad k = 1, 2, ..., 8. \tag{58}$$

In the current general context, it is difficult to demonstrate the existence of a single solution w of this equation that would lead to solve the Rayleigh wave problem formulated at the beginning of this section (here, we include conditions (57) and (58)). However, when a triple porous material is specified by its characteristics, then the secular equation (54) can be solved by specific mathematical tools, and this will be exemplified later for Berea sandstones.

The above result may be considered as most general in the sense that some other important formulas, previously established by different authors, may be deduced from our result as special cases:

Classical elasticity theory: when the porosity and thermal effects are canceled, then our results show that:

$$\begin{aligned} s_1^2 &= \frac{\upsilon^2}{c_1^2}, \quad r_1 = i\sqrt{1 - \frac{\upsilon^2}{c_1^2}}, \\ s_8^2 &= \frac{\upsilon^2}{c_2^2}, \quad r_8 = i\sqrt{1 - \frac{\upsilon^2}{c_2^2}}, \end{aligned} \tag{59}$$

and the secular equation (54) reduces to $E(r_1, s_1) = 0$, i.e.,

$$\left(2 - \frac{\upsilon^2}{c_2^2}\right)^2 = 4\sqrt{1 - \frac{\upsilon^2}{c_1^2}}\sqrt{1 - \frac{\upsilon^2}{c_2^2}}, \tag{60}$$

a relation first established by Rayleigh [50].

Classical thermoelasticity theory: when all pores have the same temperature and the effects of the pores are canceled, our results look like:

$$s_8^2 = \frac{\upsilon^2}{c_2^2}, \quad r_8 = i\sqrt{1 - \frac{\upsilon^2}{c_2^2}}, \tag{61}$$

and s_1^2 and s_5^2 are the roots of the following equation:

$$s^4 + \left[w^2 + \frac{c_1 T_0}{\varkappa K^{11}} w \left(c_{11} + \frac{\omega_1^2}{\varrho c_1^2} \right) \right] s^2 + \frac{c_1 T_0}{\varkappa K^{11}} c_{11} w^3 = 0, \tag{62}$$

and the secular equation (54) reduces to:

$$\left(s_1^2+\frac{c_1c_{11}T_0}{\varkappa K^{11}}\,w\right)(s_5^2+w^2)\left[(2-s_8^2)\left(2-\frac{c_1^2}{c_2^2}\,s_1^2\right)+4r_1r_8\right]+\frac{\omega_1^2T_0s_1^2w}{\varrho c_1\varkappa K^{11}}\left[(2-s_8^2)\left(2-\frac{c_1^2}{c_2^2}\,s_5^2\right)+4r_5r_8\right]=0, \tag{63}$$

having denoted by K^{11} the thermal conductivity, by c_{11} the heat capacity, and by ω_1 the thermal expansion coefficient for the classical thermoelastic case.

Elastic solid with triple porosity: when the thermal effects are canceled, then our results show that s_8^2 is given by relation (61), while s_1^2, s_2^2, s_3^2, and s_4^2 are the solutions of the equation:

$$\det\big(\Pi(s^2)\big)=0, \tag{64}$$

where

$$\Pi(s^2)\equiv\begin{pmatrix}\pi_{11}(s^2) & \pi_{12}(s^2) & \pi_{13}(s^2) & \pi_{14}(s^2)\\ \pi_{21}(s^2) & \pi_{22}(s^2) & \pi_{23}(s^2) & \pi_{24}(s^2)\\ \pi_{31}(s^2) & \pi_{32}(s^2) & \pi_{33}(s^2) & \pi_{34}(s^2)\\ \pi_{41}(s^2) & \pi_{42}(s^2) & \pi_{43}(s^2) & \pi_{44}(s^2)\end{pmatrix}, \tag{65}$$

and the secular equation (54) reduces to:

$$\begin{vmatrix}E(r_1,s_1) & E(r_2,s_2) & E(r_3,s_3) & E(r_4,s_4)\\ \pi_{21}^*(s_1^2) & \pi_{22}^*(s_2^2) & \pi_{23}^*(s_3^2) & \pi_{24}^*(s_4^2)\\ \pi_{31}^*(s_1^2) & \pi_{32}^*(s_2^2) & \pi_{33}^*(s_3^2) & \pi_{34}^*(s_4^2)\\ \pi_{41}^*(s_1^2) & \pi_{42}^*(s_2^2) & \pi_{43}^*(s_3^2) & \pi_{44}^*(s_4^2)\end{vmatrix}=0, \tag{66}$$

which agrees with the secular equation described in Arusoaie and Chiriţă [51].

4. Numerical simulation

In order to give practical application to the theoretical results shown in the previous section, we take into account a material like the Berea sandstone, considering for it the propagation of Rayleigh surface waves. The reference is to a sedimentary rock with grains predominantly sand-sized, made of quartz sand held together by silica, whose importance in the oil and gas industry is considerable. The Berea sandstone, a good reservoir rock in view of relatively high porosity and permeability, often finds application as a reference material in the event that the constituents of a reservoir are not known. For further details about the characteristics of Berea sandstone, the reader can refer to the book by Jaeger et al. [52], as well as to the papers by Shankland et al. [36], Davis et al. [41], Khaled et al. [53], Coyner [54], Davis [55], and Ikeda et al. [56].

The coefficients entering into the secular equation take the values:

$$c_1=2402\,\frac{\mathrm{m}}{\mathrm{s}},\quad c_2=1511\,\frac{\mathrm{m}}{\mathrm{s}},\quad \varrho=2115\,\frac{\mathrm{kg}}{\mathrm{m}^3},\quad \varkappa=1\ \mathrm{m}^{-1},\quad T_0=20^{\circ}\mathrm{C}; \tag{67}$$

$$\beta_1=0.11875,\quad \beta_2=0.95,\quad \beta_3=0.55,\quad \omega_1=-2.61\times10^4\,\frac{\mathrm{kg}}{\mathrm{ms}^2\,^{\circ}\mathrm{C}},\quad \omega_2=-1.5\times10^4\,\frac{\mathrm{kg}}{\mathrm{ms}^2\,^{\circ}\mathrm{C}},\quad \omega_3=-2.01\times10^4\,\frac{\mathrm{kg}}{\mathrm{ms}^2\,^{\circ}\mathrm{C}}; \tag{68}$$

Table 1. Solutions of the secular equations depending on the coupling conditions.

	Classical elasticity, equation (60)	Classical thermoelasticity, equation (63)
w	$-0.5700698473\,i$	$-3.6833\times10^{-9}-0.5700698853\,i$
$v=iwc_1$	$1369.30777\ m/s$	$(1369.30786-8.8472\times10^{-6}\,i)\ m/s$
	Elastic with triple porosity, eq. (66)	**Fully coupled model, equation (54)**
w	$-5.3823\times10^{-9}-0.5700710675\,i$	$-5.3847\times10^{-9}-0.5700711370\,i$
$v=iwc_1$	$(1369.31070-12.9282\times10^{-6}\,i)$ m/s	$(1369.31087-12.9342\times10^{-6}\,i)$ m/s

$$\gamma_1=0.5\,\frac{\mathrm{ms}}{\mathrm{kg}},\quad \gamma_2=0.4\,\frac{\mathrm{ms}}{\mathrm{kg}},\quad \gamma_3=0.6\,\frac{\mathrm{ms}}{\mathrm{kg}},$$
$$d_1=0.3\,\frac{\mathrm{kg}}{\mathrm{ms^3\,^\circ C}},\quad d_2=0.2\,\frac{\mathrm{kg}}{\mathrm{ms^3\,^\circ C}},\quad d_3=0.1\,\frac{\mathrm{kg}}{\mathrm{ms^3\,^\circ C}}; \tag{69}$$

$$\mathbf{A}=\begin{pmatrix}5.4 & 0.4 & 0.3\\ 0.4 & 1.35 & 0.2\\ 0.3 & 0.2 & 2\end{pmatrix}\times10^{-6}\times\frac{\mathrm{ms^2}}{\mathrm{kg}},\quad \mathbf{B}=\begin{pmatrix}-1 & 1 & 0\\ 1 & -1 & 1\\ 0 & 1 & -1\end{pmatrix}\times10^{-9}\times\frac{1}{^\circ\mathrm{C}}$$
$$\mathbf{C}=\begin{pmatrix}0.88 & 0.05 & 0.03\\ 0.05 & 0.99 & 0.04\\ 0.03 & 0.04 & 0.77\end{pmatrix}\times10^{5}\times\frac{\mathrm{kg}}{\mathrm{ms^2\,^\circ C^2}}; \tag{70}$$

$$(k^{mn})=\begin{pmatrix}24.722 & 0.01 & 0.02\\ 0.01 & 6.1806 & 0.03\\ 0.02 & 0.03 & 8.005\end{pmatrix}\times10^{-12}\times\frac{\mathrm{m^3s}}{\mathrm{kg}},$$
$$(K^{mn})=\begin{pmatrix}2.34 & -0.01 & 0.02\\ -0.01 & 2.02 & 0.03\\ 0.02 & 0.03 & 1.99\end{pmatrix}\times\frac{\mathrm{kgm}}{\mathrm{s^3\,^\circ C}}. \tag{71}$$

The secular equation (54) referred to the case of fully coupled model, as well as the secular equations (60), (63), and (66) referred to the classical elasticity, thermoelasticity, and elasticity with triple porosity sub-cases, respectively, are solved through the software package Wolfram Mathematica. The graphical results proposed are obtained by resorting to software packages Mathematica and MathWorks MATLAB. The performed analysis provides information about the main features of the Rayleigh wave solution: the speed of propagation and the exponential decrease of the amplitude, as well as the time attenuation factor.

Regarding Table 1, we can observe that it involves important effects on the essential characteristics of the Rayleigh wave propagation: (1) the propagation speed and (2) the attenuation of the amplitude in time. Actually, it suggest that (1) the coupling of the mechanical deformations with the thermal processes produces an increase of the propagation velocity for the Rayleigh waves, corroborated with the appearance of the attenuation in time of their amplitude; (2) the coupling of the mechanical deformations with the pore system also turns into an increase of the speed of propagation for the Rayleigh waves, corroborated with the appearance of the attenuation in time of their amplitude; and (3) the coupling of mechanical deformations with both pore system and thermal imbalance leads to a significant increase in the propagation velocity of the Rayleigh waves and to an increase of their amplitude attenuation, even in relation to the former results (points 1 and 2).

Figures 1–4 highlight, each of them, the graphical position of the solution w of the secular equation for the corresponding coupled cases in question. Concerning the involved pictures, we outline some technical observations on the graphical results proposed.

Figure 1 is referred to the classical thermoelastic case: it is a purely analytical plot obtained through the Mathematica Plot3D tool. Figure 2 is referred to the elastic case with triple porosity: given the complexity of the related secular equation, it is obtained by creating an appropriate (Re(w), Im(w)) grid,

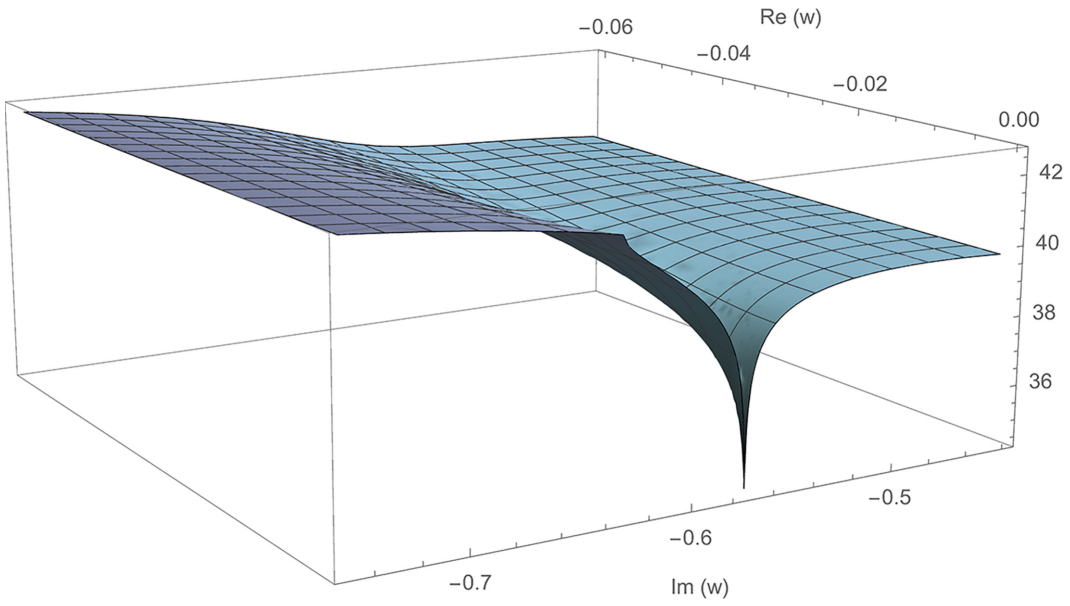

Figure 1. Classical thermoelastic case. Mathematica Plot3D of $Log\,|\Upsilon(w)|$, being $\Upsilon(w)$ the LHS of the secular equation (63), versus $Re(w)$, $Im(w)$.

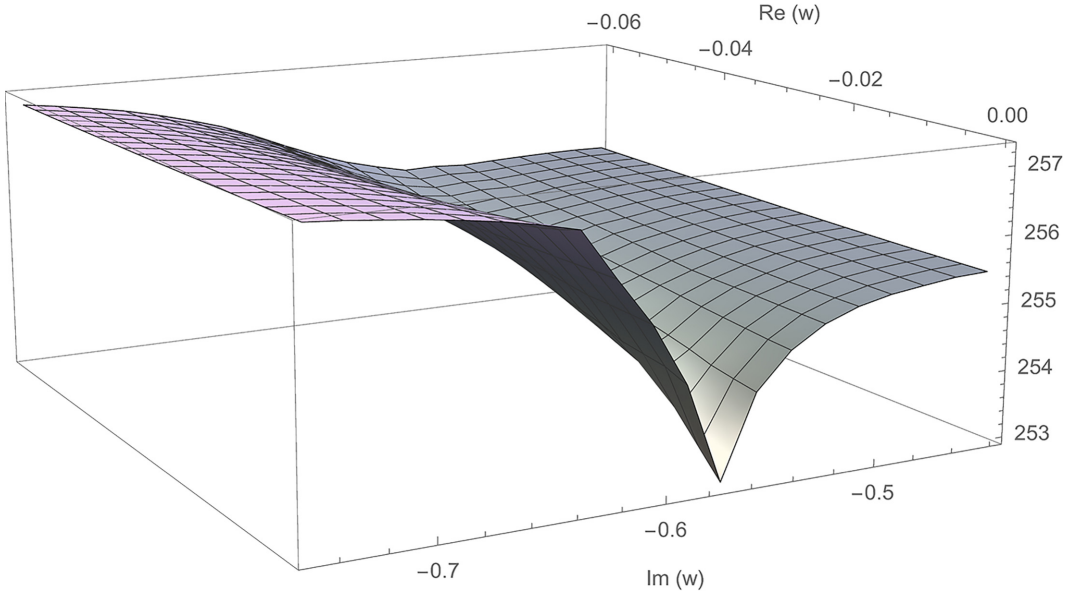

Figure 2. Elastic case with triple porosity. Mathematica ListPlot3D of $Log\,|\mathbf{\Phi}(w)|$, being $\mathbf{\Phi}(w)$ the LHS of the secular equation (66), versus Re(w), Im(w).

and then representing the numerical results through the Mathematica ListPlot3D tool. Figures 3 and 4 are referred to the fully coupled model: in this case, the level of complexity of the secular equation is even greater, which is why in addition to the discretization of the data, as in the case of Figure 2, it is necessary to proceed as follows. A two-dimensional (2D) version of the result is obtained through the Mathematica ListContourPlot tool while, with regard to its three-dimensional (3D)-counterpart, purely technical limitations of the machine force the use of the MATLAB plot3 tool, with a clearly improved graphic rendering. As for the discretization process, it is important to underline that all the numerical

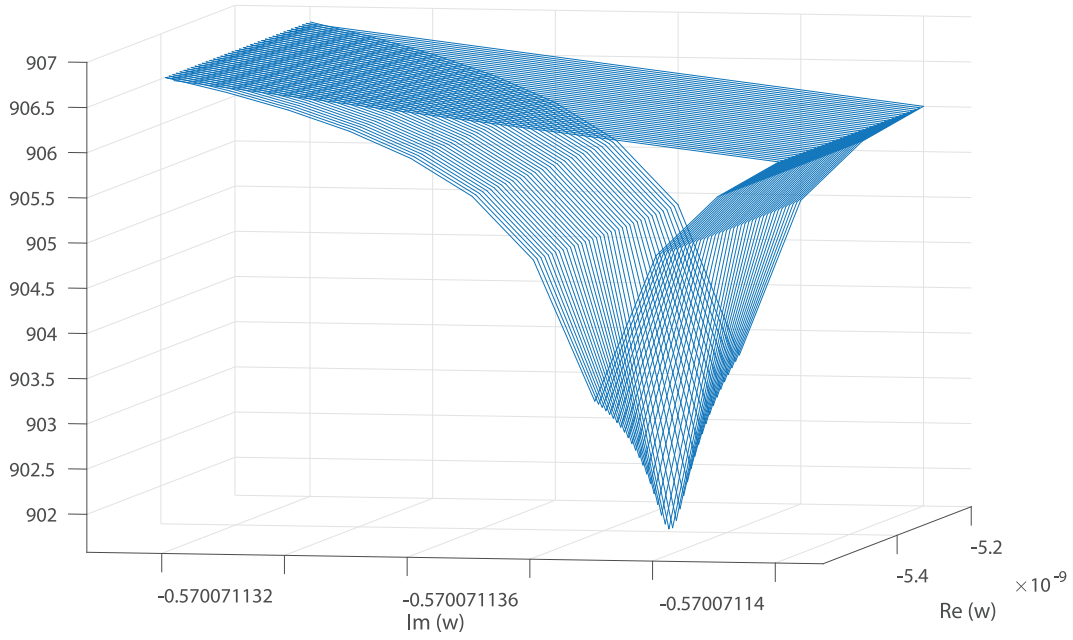

Figure 3. Fully coupled case. MATLAB plot3 of $Log|\Psi(w)|$, being $\Psi(w)$ the LHS of the secular equation (54), versus Re(w), Im(w).

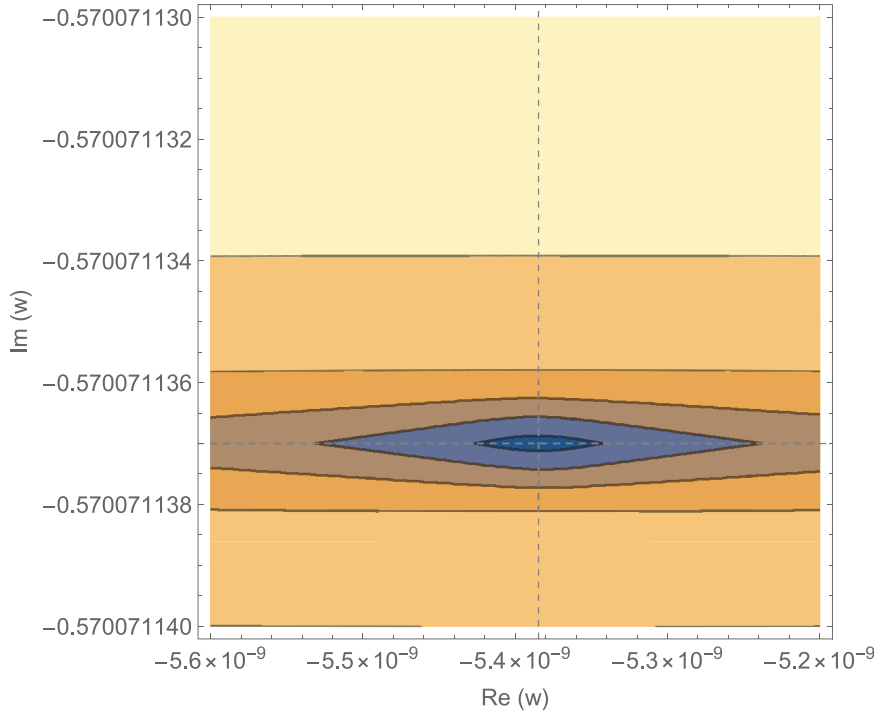

Figure 4. Fully coupled case. Mathematica ListContourPlot of $Log|\Psi(w)|$, being $\Psi(w)$ the LHS of the secular equation (54), versus Re(w), Im(w). Highlighted with dashed lines the numerical values detectable in Table 1 and related to the fully coupled case.

data are obtained using the software package Mathematica: in particular, to be more explicit, Figures 3 and 4 refer to exactly the same set of numerical data.

Concluding, it is worth underline that the above simulations bring to light the following important phenomena: (1) an increase in the velocity of propagation for the Rayleigh wave solution,

simultaneously with the emergence of the time exponential decrease of its amplitude and (2) a slower attenuation in time of the amplitude of the Rayleigh wave solution.

5. Final discussions

This paper provides mathematical results regarding the propagation of Rayleigh waves in an elastic material with triple porosity and local thermal imbalance, culminating in the establishment of a complex secular equation. It also shows how numerical methods, Mathematica and MATLAB software packages, can be used in solving the secular equation to discover the effects of coupling mechanical deformation with thermal processes and pore systems. A significant illustrative example is chosen regarding the simulation of the results on a material such as Berea sandstone, highlighting the consequences of accounting for the thermal effects and pore systems on the speed of propagation of the Rayleigh wave and on the damping over time of its amplitude.

When a triple porous medium in local thermal non-equilibrium is taken into account, then friction phenomena and heat transfer processes, in combination with the presence of fluid flows at level of macro-, meso-, and micro-pores, appear to be mechanisms able to cause an attenuation in time of the Rayleigh wave solutions. In particular, with regard to the mechanical friction, it happens that part of the kinetic energy from the elastic wave is converted in thermal energy: clearly, this energy is not lost, but has the effect of slightly raising the temperature of the medium. In addition, considering the skeleton/fluid thermal exchanges at the level of macro- and micro-pores, the Rayleigh wave solution results attenuated over time. On the other side, the secular relation (54) shows a close connection between mechanical, thermal, and porosity effects on the Rayleigh wave solution. In fact, the fluid flow oscillations inside the pores induce an increase of the propagation velocity for the Rayleigh surface wave, in parallel with a decrease in time of its amplitude. Our investigation provides thus interesting information about the Rayleigh wave propagation problem when interactions between elastic structure, triple porosity, and local thermal effects are considered. In this context, the results of the various mechanical couplings with the thermal ones and with the pore systems are compared, highlighting the increase of the propagation speed of the Rayleigh wave and the appearance of the amortization in time of its amplitude.

Finally, we note that, although the thermo-mechanical model in question is quite complex (based on a system consisting of nine differential equations: three hyperbolic and six parabolic), the methodology developed by us, by looking for wave solutions with assigned wavelength, manages to establish the secular equation in the form of an algebraic equation involving a seventh-order determinant. It allows the rediscovery of previous results regarding simpler mechanical models, such as classical thermoelasticity and elastic triple porosity.

Although the problem treated is substantially theoretical, we are confident that it can give useful information to experimenters and researchers working in the geophysical field, as well as to seismologists interested in mining earthquakes and fractured reservoirs.

Funding

The author(s) disclosed receipt of the following financial support for the research, authorship, and/or publication of this article: V.Z. acknowledges the GNFM (Italian National Group of Mathematical Physics, INdAM) for supporting his research activity; S.C. acknowledges a support from the Project STARDUST-R H2020-MSCA-ITN-2018, Grant Agreement number 813644, Al. I. Cuza University of Iaşi.

ORCID iDs

Vittorio Zampoli https://orcid.org/0000-0001-5395-2089
Stan Chiriţă https://orcid.org/0000-0001-7560-0367

References

[1] Heller-Kallai, L. Chapter 10.2—thermally modified clay minerals. *Dev Clay Sci* 2013; 5: 411–433.
[2] Biot, MA. General theory of three-dimensional consolidation. *J Appl Phys* 1941; 12(2): 155–164.
[3] Biot, MA. Theory of elasticity and consolidation for a porous anisotropic solid. *J Appl Phys* 1955; 26(2): 182–185.

[4] Biot, MA. General solutions of the equations of elasticity and consolidation for a porous material. *J Appl Mech* 1956; 23(1): 91–96.
[5] Biot, MA. Theory of propagation of elastic waves in a fluid-saturated porous solid. *J Acous Soc Am* 1956; 28(2): 168–191.
[6] Cheng, AH-D. *Poroelasticity*. Cham: Springer International Publishing AG, 2016.
[7] Straughan, B. *Mathematical Aspects of Multi-Porosity Continua* (Advances in Mechanics and Mathematics), vol. 38. Cham: Springer International Publishing AG, 2017.
[8] Svanadze, M. *Potential Method in Mathematical Theories of Multi-Porosity Media* (Interdisciplinary Applied Mathematics), vol. 51. Cham: Springer International Publishing AG, 2019.
[9] Barenblatt, GI, Zheltov, YP, and Kochina, IN. Basic concepts in the theory of seepage of homogeneous liquids in fissured rocks (strata). *J Appl Math Mech* 1960; 24(5): 1286–1303.
[10] Barenblatt, GI. On certain boundary-value problems for the equations of seepage of a liquid in fissured rocks. *J Appl Math Mech* 1963; 27(2): 513–518.
[11] Wilson, RK, and Aifantis, EC. On the theory of consolidation with double porosity. *Int J Eng Sci* 1982; 20(9): 1009–1035.
[12] Wilson, RK, and Aifantis, EC. A double porosity model for acoustic wave propagation in fractured-porous rock. *Int J Eng Sci* 1984; 22(8–10): 1209–1217.
[13] Beskos, DE. Dynamics of saturated rocks. I: equations of motion. *J Eng Mech ASCE* 1989; 115(5): 982–995.
[14] Beskos, DE, Vgenopoulou, I, and Providakis, CP. Dynamics of saturated rocks. II: body waves. *J Eng Mech ASCE* 1989; 115(5): 996–1016.
[15] Beskos, DE, and Papadakis, CN. Dynamics of saturated rocks. III: Rayleigh waves. *J Eng Mech ASCE* 1989; 115(5): 1017–1034.
[16] Vgenopoulou, I, and Beskos, DE. Dynamics of saturated rocks. IV: column and borehole problems. *J Eng Mech ASCE* 1992; 118(9): 1795–1813.
[17] Auriault, JL, and Boutin, C. Deformable porous media with double porosity III: acoustics. *Transp Porous Media* 1994; 14: 143–162.
[18] Olny, X, and Boutin, C. Acoustic wave propagation in double porosity media. *J Acous Soc Am* 2003; 114(1): 73–89.
[19] Boutin, C, and Royer, P. On models of double porosity poroelastic media. *Geophys J Int* 2015; 203(3): 1694–1725.
[20] Pride, SR, and Berryman, JG. Linear dynamics of double-porosity dual-permeability materials. I. Governing equations and acoustic attenuation. *Physical Review E* 2003; 68: 036603.
[21] Pride, SR, and Berryman, JG. Linear dynamics of double-porosity dual-permeability materials. II. Fluid transport equations. *Physical Review E* 2003; 68: 036604.
[22] Al-Ahmadi, HA. *A triple-porosity model for fractured horizontal wells*. Master's Thesis, Texas A&M University, 2010, http://hdl.handle.net/1969.1/ETD-TAMU-2010-08-8545
[23] Al-Ahmadi, HA, and Wattenbarger, RA. Triple-porosity models: one further step towards capturing fractured reservoirs heterogeneity. In: *SPE/DGS Saudi Arabia section technical symposium and exhibition*, Al-Khobar, Saudi Arabia, 15–18 May 2011. Richardson, TX: Society of Petroleum Engineers.
[24] Tivayanonda, V, Apiwathanasorn, S, Economides, C, et al. Alternative interpretations of shale Gas/Oil rate behavior using a triple porosity model. In: *Paper presented at the SPE annual technical conference and exhibition*, San Antonio, TX, 8–10 October 2012, SPE-159703-MS. Richardson, TX: Society of Petroleum Engineers.
[25] Deng, JH, Leguizamon, JA, and Aguilera, R. Petrophysics of triple-porosity tight gas reservoirs with a link to gas productivity. *SPE Res Eval Eng* 2011; 14(5): 566–577.
[26] Shackelford, CD. Contaminant transport. In: Daniel, DE (ed.) *Geotechnical practice for waste disposal*. Boston, MA: Springer, 1993, pp. 33–65.
[27] Gwo, JP, Jardine, PM, Wilson, GV, et al. A multiple-pore-region concept to modeling mass transfer in subsurface media. *J Hydrol* 1995; 164: 217–237.
[28] Moutsopoulos, KN, Konstantinidis, AA, Meladiotis, I, et al. Hydraulic behavior and contaminant transport in multiple porosity media. *Transp Porous Media* 2001; 42: 265–292.
[29] Giorgio, I, Andreaus, U, and Madeo, A. The influence of different loads on the remodeling process of a bone and bioresorbable material mixture with voids. *Continuum Mech Thermodyn* 2016; 28: 21–40.
[30] Giorgio, I, Spagnuolo, M, Andreaus, U, et al. In-depth gaze at the astonishing mechanical behavior of bone: a review for designing bio-inspired hierarchical metamaterials. *Math Mech Solids* 2021; 26(7): 1074–1103.
[31] Müller, TM, Gurevich, B, and Lebedev, M. Seismic wave attenuation and dispersion resulting from wave-induced flow in porous rocks—a review. *Geophysics* 2010; 75(5): A147–A164.
[32] Pride, SR. Relationships between seismic and hydrological properties. In: Rubin, Y, and Hubbard, SS (eds) *Hydrogeophysics*. *Water Science and Technology Library*, vol. 50. Dordrecht: Springer, 2005, pp. 253–290.
[33] Parotidis, M, Rothert, E, and Shapiro, SA. Pore-pressure diffusion: a possible triggering mechanism for the earthquake swarms 2000 in Vogtland/NW-Bohemia, central Europe. *Geophys Res Lett* 2003; 30(20): 2075.
[34] Biot, MA. Mechanics of deformation and acoustic propagation in porous media. *J Appl Phys* 1962; 33: 1482–1498.
[35] Biot, MA. Generalized theory of acoustic propagation in porous dissipative media. *J Acous Soc Am* 1962; 34(9): 1254–1264.

[36] Shankland, TJ, Johnson, PA, and Hopson, TM. Elastic wave attenuation and velocity of Berea sandstone measured in the frequency domain. *Geophys Res Lett* 1993; 20(5): 391–394.
[37] Berryman, JG, and Wang, HF. Elastic wave propagation and attenuation in a double-porosity dual-permeability medium. *Int J Rock Mech Min Sci* 2000; 37(1–2): 63–78.
[38] Svanadze, M. Plane waves and boundary value problems in the theory of elasticity for solids with double porosity. *Acta Applicandae Mathematicae* 2012; 122: 461–471.
[39] Ciarletta, M, Passarella, F, and Svanadze, M. Plane waves and uniqueness theorems in the coupled linear theory of elasticity for solids with double porosity. *J Elast* 2014; 114: 55–68.
[40] Straughan, B. Waves and uniqueness in multi-porosity elasticity. *J Therm Stres* 2016; 39(6): 704–721.
[41] Davis, ES, Sturtevant, BT, Sinha, DN, et al. Resonant ultrasound spectroscopy studies of Berea sandstone at high temperature. *J Geophys Res Solid Earth* 2016; 121(9): 6401–6410.
[42] Galeş, C, and Chiriţă, S. Wave propagation in materials with double porosity. *Mech Mater* 2020; 149: 103558.
[43] Chiriţă, S, and Arusoaie, A. Thermoelastic waves in double porosity materials. *European J Mech—A/Solids* 2021; 86: 104177.
[44] Chiriţă, S, and Galeş, C. Wave propagation and attenuation in time in local thermal non-equilibrium triple porosity thermoelastic medium. *Acta Mechanica* 2021; 232: 4217–4233.
[45] Nield, DA. A note on modelling of local thermal non-equilibrium in a structured porous medium. *International Journal Heat and Mass Transfer* 2002; 45(21): 4367–4368.
[46] Franchi, F, Lazzari, B, Nibbi, R, et al. Uniqueness and decay in local thermal non-equilibrium double porosity thermoelasticity. *Math Meth Appl Sci* 2018; 41(16): 6763–6771.
[47] Svanadze, M. On the linear theory of double porosity thermoelasticity under local thermal nonequilibrium. *J Therm Stres* 2019; 42(7): 890–913.
[48] Chiriţă, S. Modeling triple porosity under local thermal nonequilibrium. *J Therm Stres* 2020; 43(2): 210–224.
[49] Kaplunov, J, and Prikazchikov, DA. Chapter one—asymptotic theory for Rayleigh and Rayleigh-type waves. *Advances in Applied Mechanics* 2017; 50: 1–106.
[50] Rayleigh, L. On waves propagated along the plane surface of an elastic solid. *Proc London Math Soc* 1885; s1-17: 4–11.
[51] Arusoaie, A, and Chiriţă, S. Waves in the theory of elasticity for triple porosity materials. *Meccanica* 2022; 57(3): 641–657.
[52] Jaeger, JC, Cook, NGW, and Zimmerman, RW. *Fundamentals of rock mechanics*. 4th ed. Malden: Blackwell Publishing, 2007.
[53] Khaled, MY, Beskos, DE, and Aifantis, EC. On the theory of consolidation with double porosity-III: a finite element formulation. *Int J Num Anal Meth Geomech* 1984; 8(2): 101–123.
[54] Coyner, KB. *Effects of stress, pore pressure, and pore fluids on bulk strain, velocity, and permeability of rocks*. PhD Thesis, Massachusetts Institute of Technology, Cambridge, MA, 1984, https://dspace.mit.edu/handle/1721.1/15367
[55] Davis, ES. *Anomalous elastic behavior in Berea sandstone*. PhD Thesis, University of Houston, Houston, TX, 2018.
[56] Ikeda, K, Goldfarb, E, and Tisato, N. Calculating effective elastic properties of Berea sandstone using the segmentation-less method without targets. *J Geophys Res Solid Earth* 2020; 125(6): e2019JB018680.

Appendix I

The elements of matrix $\pi(s^2)$

The elements of the matrix $\pi(s^2)$ are defined as follows:

$$\begin{aligned}
&\pi_{11}(s^2)=s^2+w^2,\quad \pi_{12}(s^2)=\frac{\beta_1 s^2}{c_1\sqrt{\varrho a_{11}}},\quad \pi_{13}(s^2)=\frac{\beta_2 s^2}{c_1\sqrt{\varrho a_{22}}},\\
&\pi_{14}(s^2)=\frac{\beta_3 s^2}{c_1\sqrt{\varrho a_{33}}},\quad \pi_{15}(s^2)=\frac{\omega_1 T_0 s^2}{\varrho c_1^2},\quad \pi_{16}(s^2)=\frac{\omega_2 T_0 s^2}{\varrho c_1^2},\quad \pi_{17}(s^2)=\frac{\omega_3 T_0 s^2}{\varrho c_1^2};
\end{aligned}\tag{72}$$

$$\begin{aligned}
&\pi_{21}(s^2)=-\frac{\beta_1}{\varkappa k^{11}}\sqrt{\frac{a_{11}}{\varrho}}w,\quad \pi_{22}(s^2)=s^2+\frac{D_{11}}{\varkappa^2 k^{11}}+\frac{a_{11}c_1}{\varkappa k^{11}}w,\quad \pi_{23}(s^2)=\left(\frac{k^{12}}{k^{11}}s^2\right.\\
&\left.+\frac{D_{12}}{\varkappa^2 k^{11}}+\frac{a_{12}c_1}{\varkappa k^{11}}w\right)\sqrt{\frac{a_{11}}{a_{22}}},\quad \pi_{24}(s^2)=\left(\frac{k^{13}}{k^{11}}s^2+\frac{D_{13}}{\varkappa^2 k^{11}}+\frac{a_{13}c_1}{\varkappa k^{11}}w\right)\sqrt{\frac{a_{11}}{a_{33}}},\\
&\pi_{25}(s^2)=\frac{b_{11}T_0}{\varkappa k^{11}}\sqrt{\frac{a_{11}}{\varrho}}w,\quad \pi_{26}(s^2)=\frac{b_{12}T_0}{\varkappa k^{11}}\sqrt{\frac{a_{11}}{\varrho}}w,\quad \pi_{27}(s^2)=\frac{b_{13}T_0}{\varkappa k^{11}}\sqrt{\frac{a_{11}}{\varrho}}w;
\end{aligned}\tag{73}$$

$$\pi_{31}(s^2) = -\frac{\beta_2}{\varkappa k^{22}}\sqrt{\frac{a_{22}}{\varrho}}w, \quad \pi_{32}(s^2) = \left(\frac{k^{21}}{k^{22}}s^2 + \frac{D_{21}}{\varkappa^2 k^{22}} + \frac{a_{21}c_1}{\varkappa k^{22}}w\right)\sqrt{\frac{a_{22}}{a_{11}}}, \quad \pi_{33}(s^2)$$
$$= s^2 + \frac{D_{22}}{\varkappa^2 k^{22}} + \frac{a_{22}c_1}{\varkappa k^{22}}w, \quad \pi_{34}(s^2) = \left(\frac{k^{23}}{k^{22}}s^2 + \frac{D_{23}}{\varkappa^2 k^{22}} + \frac{a_{23}c_1}{\varkappa k^{22}}w\right)\sqrt{\frac{a_{22}}{a_{33}}}, \tag{74}$$
$$\pi_{35}(s^2) = \frac{b_{21}T_0}{\varkappa k^{22}}\sqrt{\frac{a_{22}}{\varrho}}w, \quad \pi_{36}(s^2) = \frac{b_{22}T_0}{\varkappa k^{22}}\sqrt{\frac{a_{22}}{\varrho}}w, \quad \pi_{37}(s^2) = \frac{b_{23}T_0}{\varkappa k^{22}}\sqrt{\frac{a_{22}}{\varrho}}w;$$

$$\pi_{41}(s^2) = -\frac{\beta_3}{\varkappa k^{33}}\sqrt{\frac{a_{33}}{\varrho}}w, \quad \pi_{42}(s^2) = \left(\frac{k^{31}}{k^{33}}s^2 + \frac{D_{31}}{\varkappa^2 k^{33}} + \frac{a_{31}c_1}{\varkappa k^{33}}w\right)\sqrt{\frac{a_{33}}{a_{11}}},$$
$$\pi_{43}(s^2) = \left(\frac{k^{32}}{k^{33}}s^2 + \frac{D_{32}}{\varkappa^2 k^{33}} + \frac{a_{32}c_1}{\varkappa k^{33}}w\right)\sqrt{\frac{a_{33}}{a_{22}}}, \quad \pi_{44}(s^2) = s^2 + \frac{D_{33}}{\varkappa^2 k^{33}} + \frac{a_{33}c_1}{\varkappa k^{33}}w, \tag{75}$$
$$\pi_{45}(s^2) = \frac{b_{31}T_0}{\varkappa k^{33}}\sqrt{\frac{a_{33}}{\varrho}}w, \quad \pi_{46}(s^2) = \frac{b_{32}T_0}{\varkappa k^{33}}\sqrt{\frac{a_{33}}{\varrho}}w, \quad \pi_{47}(s^2) = \frac{b_{33}T_0}{\varkappa k^{33}}\sqrt{\frac{a_{33}}{\varrho}}w;$$

$$\pi_{51}(s^2) = -\frac{\omega_1 c_1 w}{\varkappa K^{11}}, \quad \pi_{52}(s^2) = \frac{b_{11}c_1^2}{\varkappa K^{11}}\sqrt{\frac{\varrho}{a_{11}}}w, \quad \pi_{53}(s^2) = \frac{b_{12}c_1^2}{\varkappa K^{11}}\sqrt{\frac{\varrho}{a_{22}}}w,$$
$$\pi_{54}(s^2) = \frac{b_{13}c_1^2}{\varkappa K^{11}}\sqrt{\frac{\varrho}{a_{33}}}w, \quad \pi_{55}(s^2) = s^2 + \frac{d_{11}}{\varkappa^2 K^{11}} + \frac{c_{11}c_1T_0}{\varkappa K^{11}}w, \tag{76}$$
$$\pi_{56}(s^2) = \frac{K^{12}}{K^{11}}s^2 + \frac{d_{12}}{\varkappa^2 K^{11}} + \frac{c_{12}c_1T_0}{\varkappa K^{11}}w, \quad \pi_{57}(s^2) = \frac{K^{13}}{K^{11}}s^2 + \frac{d_{13}}{\varkappa^2 K^{11}} + \frac{c_{13}c_1T_0}{\varkappa K^{11}}w;$$

$$\pi_{61}(s^2) = -\frac{\omega_2 c_1 w}{\varkappa K^{22}}, \quad \pi_{62}(s^2) = \frac{b_{21}c_1^2}{\varkappa K^{22}}\sqrt{\frac{\varrho}{a_{11}}}w, \quad \pi_{63}(s^2) = \frac{b_{22}c_1^2}{\varkappa K^{22}}\sqrt{\frac{\varrho}{a_{22}}}w,$$
$$\pi_{64}(s^2) = \frac{b_{23}c_1^2}{\varkappa K^{22}}\sqrt{\frac{\varrho}{a_{33}}}w, \quad \pi_{65}(s^2) = \frac{K^{21}}{K^{22}}s^2 + \frac{d_{21}}{\varkappa^2 K^{22}} + \frac{c_{21}c_1T_0}{\varkappa K^{22}}w, \tag{77}$$
$$\pi_{66}(s^2) = s^2 + \frac{d_{22}}{\varkappa^2 K^{22}} + \frac{c_{22}c_1T_0}{\varkappa K^{22}}w, \quad \pi_{67}(s^2) = \frac{K^{23}}{K^{22}}s^2 + \frac{d_{23}}{\varkappa^2 K^{22}} + \frac{c_{23}c_1T_0}{\varkappa K^{22}}w;$$

$$\pi_{71}(s^2) = -\frac{\omega_3 c_1 w}{\varkappa K^{33}}, \quad \pi_{72}(s^2) = \frac{b_{31}c_1^2}{\varkappa K^{33}}\sqrt{\frac{\varrho}{a_{11}}}w, \quad \pi_{73}(s^2) = \frac{b_{32}c_1^2}{\varkappa K^{33}}\sqrt{\frac{\varrho}{a_{22}}}w,$$
$$\pi_{74}(s^2) = \frac{b_{33}c_1^2}{\varkappa K^{33}}\sqrt{\frac{\varrho}{a_{33}}}w, \quad \pi_{75}(s^2) = \frac{K^{31}}{K^{33}}s^2 + \frac{d_{31}}{\varkappa^2 K^{33}} + \frac{c_{31}c_1T_0}{\varkappa K^{33}}w, \tag{78}$$
$$\pi_{76}(s^2) = \frac{K^{32}}{K^{33}}s^2 + \frac{d_{32}}{\varkappa^2 K^{33}} + \frac{c_{32}c_1T_0}{\varkappa K^{33}}w, \quad \pi_{77}(s^2) = s^2 + \frac{d_{33}}{\varkappa^2 K^{33}} + \frac{c_{33}c_1T_0}{\varkappa K^{33}}w.$$